Cell Host & Microbe
Article

A Highly Structured, Nuclease-Resistant, Noncoding RNA Produced by Flaviviruses Is Required for Pathogenicity

Gorben P. Pijlman,[1,4,5] Anneke Funk,[1,4] Natasha Kondratieva,[1] Jason Leung,[1] Shessy Torres,[1] Lieke van der Aa,[1] Wen Jun Liu,[1] Ann C. Palmenberg,[2] Pei-Yong Shi,[3,6] Roy A. Hall,[1] and Alexander A. Khromykh[1,*]
[1]School of Molecular and Microbial Sciences, The University of Queensland, Brisbane, Queensland 4072, Australia
[2]Institute for Molecular Virology, University of Wisconsin, 1525 Linden Drive, Madison, WI 53706, USA
[3]Wadsworth Center, New York State Department of Health and Department of Biomedical Sciences, State University of New York, Box 22002, Albany, NY 12201-2002, USA
[4]These authors contributed equally to this work
[5]Present address: Laboratory of Virology, Wageningen University, Binnenhaven 11, 6709PD, Wageningen, The Netherlands
[6]Novartis Institute for Tropical Diseases, 10 Biopolis Road, #05-01 Chromos, 138670, Singapore
*Correspondence: a.khromykh@uq.edu.au
DOI 10.1016/j.chom.2008.10.007

SUMMARY

Viral noncoding RNAs have been shown to play an important role in virus-host interplay to facilitate virus replication. We report that members of the genus Flavivirus, a large group of medically important encephalitic RNA viruses, produce a unique and highly structured noncoding RNA of 0.3–0.5 kb derived from the 3′ untranslated region of the viral genome. Using West Nile virus as a model, we show that this subgenomic RNA is a product of incomplete degradation of viral genomic RNA by cellular ribonucleases. Highly conserved RNA structures located at the beginning of the 3′ untranslated region render this RNA resistant to nucleases, and the resulting subgenomic RNA product is essential for virus-induced cytopathicity and pathogenicity. Thus, flaviviruses evolved a unique strategy to generate a noncoding RNA product that allows them to kill the host more efficiently.

INTRODUCTION

Arthropod-borne Flaviviruses such as West Nile (WNV), dengue (DENV), Yellow fever (YFV), Tick-borne encephalitis (TBEV), and Japanese encephalitis (JEV) cause major outbreaks of potentially fatal diseases and affect more than 50 million people every year. The highly pathogenic North American strain of WNV (WNV_{NY99}) has already claimed more than 1,000 lives with more than 27,000 cases reported since its emergence in New York in 1999. In contrast, the closely related Australian strain of WNV, Kunjin (WNV_{KUN}), is highly attenuated and does not cause overt disease in humans and animals (Hall et al., 2002). The ~11 kb positive-stranded flavivirus RNA genome consists of 5′ and 3′ untranslated regions (UTRs) and one open reading frame, which encodes 10 viral proteins required for the viral life cycle (Liu et al., 2002, 2003, 2004, 2005, 2006; Westaway et al., 2003). Flavivirus UTRs are involved in translation and initiation of RNA replication and likely determine genome packaging (Markoff, 2003; Westaway et al., 2002). In addition to full-length genomic RNA (gRNA), an abundant RNA species of about 0.5 kb derived from the 3′UTR has been detected in cells infected with mosquito-borne encephalitic flaviviruses Murray Valley encephalitis (MVE) (Urosevic et al., 1997), JEV (Lin et al., 2004), and WNV (Scherbik et al., 2006). However, the mechanism of its generation and function in the viral replication cycle remained unknown.

Processing bodies (PBs, also known as GW bodies) are discrete cytoplasmic granules in which mRNA degradation, mRNA surveillance, translational repression, and RNA-mediated gene silencing take place (Eulalio et al., 2007). mRNA degradation can occur through two distinct pathways: (1) deadenylation followed by degradation through 3′-5′decay mediated by the exosome and (2) decapping and degradation by a 5′-to-3′ exonucleolytic process (Tourriere et al., 2002; Wilusz et al., 2001). The latter occurs primarily in PBs in which mRNAs are decapped by Dcp1/2 and subsequently degraded by the 5′-3′ exoribonuclease XRN1 (Sheth and Parker, 2003). XRN1 is a processive enzyme hydrolyzing RNA from the 5′ to 3′ end and an essential component of cellular mRNA decay machinery (Sheth and Parker, 2003; Stevens, 2001). Interestingly, flavivirus gRNA has no 3′poly(A) tail but a cap at the 5′ end that may target it to PBs for decapping and XRN1-mediated decay.

For the yeast homolog Xrn1p, it has been shown that certain structures in the target RNA influence efficiency of 5′-3′ exoribonucleolytic hydrolysis (Poole and Stevens, 1997). The 3′UTR of flaviviruses contains a number of highly structured regions, for some of which functions have been assigned (Markoff, 2003; Proutski et al., 1999), while no functions have been determined for other highly structured regions. Here, we show that the accumulation of a subgenomic 3′UTR-derived RNA is a specific feature of members of the flavivirus genus, and, using West Nile virus as a model, we demonstrate that this subgenomic flavivirus RNA (sfRNA) is generated as a product of gRNA degradation presumably by XRN1 exoribonuclease. We also provide evidence that the production of sfRNA is likely to be a result of XRN1 stalling mediated by rigid, conserved RNA structures in the 5′ end of the 3′UTR. Importantly, we demonstrate that sfRNA has a role in facilitating efficient virus replication and virus-induced cytopathicity in cell culture and in determining viral pathogenicity in mice.

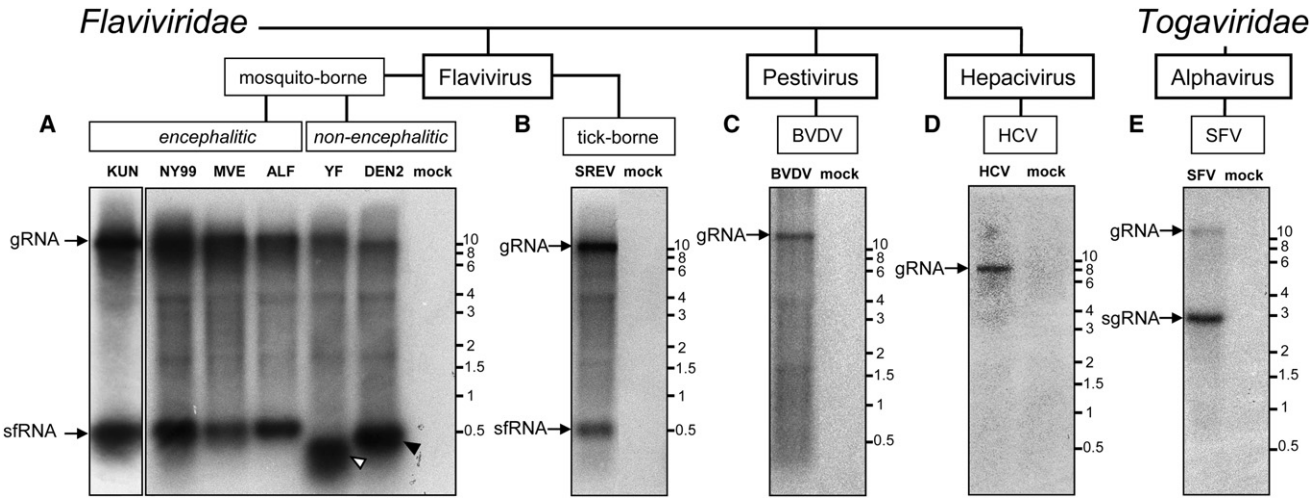

Figure 1. Flaviviruses Produce a Subgenomic RNA Species in Infected Cells

Cells were either infected with indicated viruses or transfected with replicon RNAs and analyzed for accumulation of virus-specific RNA species by northern blot hybridization detecting the 3′UTR.

(A) WNV subtype Kunjin (KUN), WNV strain NY99 (NY99), Murray Valley (MVE), Alfuy (ALF), Yellow Fever (YFV), dengue 2 replicon (DEN2); all RNAs isolated from infected/transfected BHK-21 cells.

(B) Samaurez Reef virus (SREV); RNA from infected PS-EK cells.

(C) Bovine viral diarrhea virus (BVDV); RNA from infected MDBK cells.

(D) Hepatitis C virus (HCV); RNA from HCV replicon-transfected Huh7 cells.

(E) Semliki Forest virus (SFV); RNA from SFV replicon RNA-transfected BHK-21 cells. sgRNA represents SFV subgenomic RNA produced from internal 26S promoter.

Arrowheads indicate sfRNA produced by YFV (open) and DEN2 (solid). RNA size markers (kb) are indicated.

RESULTS

Accumulation of Subgenomic RNA Is a Unique Feature of the Genus Flavivirus, Is Not Cell-Type Specific, and Is Not a Result of RNA Self-Cleavage

To investigate whether the production of subgenomic RNA species is common for all flaviviruses, cells were either infected with different viruses or electroporated with their replicon RNAs. Northern hybridizations with the corresponding 3′UTR-specific probes showed that cells infected with mosquito-borne WNV_{KUN}, WNV_{NY99}, MVEV, Alfuy (ALFV), and tick-borne Samaurez Reef virus (SREV) all produced a subgenomic RNA of similar size (~0.5 kb), while YFV-infected cells and a replicon of DENV type 2 (DENV2) produced slightly smaller RNAs (~0.3 and ~0.4 kb, respectively), correlating with the corresponding 3′UTR sizes (Figures 1A and 1B). In contrast, cells infected with viruses from other *Flaviviridae* genera, bovine viral diarrhea virus (BVDV; Pestiviruses) and (a replicon of) hepatitis C virus (HCV; Hepaciviruses), did not produce a subgenomic, 3′UTR-derived RNA (Figures 1C and 1D). Production of small subgenomic RNA was also not detected for a replicon of the unrelated Semliki Forest virus (SFV; *Togaviridae*, Alphaviruses) (Figure 1E). Taken together, the results show that generation of the subgenomic, 3′UTR-derived RNA is restricted to and conserved in the Flavivirus genus of the *Flaviviridae* family; thus, we designated it as subgenomic flavivirus RNA (sfRNA). Further analysis of sfRNA production by WNV_{KUN} showed that it is produced in abundant amounts in all cell types tested, including those of vertebrate (human, primate, and rodent) and invertebrate (mosquito) origin (Figure S1A available online). In addition, sfRNA was shown to be produced in WNV_{KUN}-infected mouse brain but was not packaged into virions and not a product of RNA self-cleavage in vitro under the conditions used (Figure S1B), clearly indicating the involvement of host or viral proteins in sfRNA generation.

Generation of sfRNA Does Not Require Viral RNA Replication, Viral Proteins, or 5′UTR

To further elucidate the mechanism of sfRNA generation, we investigated whether the production of sfRNA was dependent on viral RNA replication, expression of viral proteins, or presence of the 5′UTR. Experiments with WNV_{KUN} RNA or cDNA clones producing RNAs containing various deletions in the viral genome from a CMV promoter (Figure 2A and Supplemental Data) showed that sfRNA could be readily detected in cells transfected with all deletion constructs, replicating (KUNrep and pKUNrep2-βgal) or nonreplicating (all remaining constructs) (Figures 2B, 2C, and 2D and Supplemental Data), thus demonstrating that RNA replication, viral proteins, or the 5′UTR are not essential for sfRNA generation. The results clearly showed that cellular proteins/factors rather than viral proteins are responsible for sfRNA production.

sfRNA Is a Product of Incomplete Degradation of Genomic RNA by a Cellular Ribonuclease

Having excluded the role of viral factors in sfRNA generation and taking into account that sfRNA represents the 3′-terminal product of genomic RNA, we hypothesized that a cellular ribonuclease with 5′-3′ RNA hydrolyzing activity may be responsible for its generation. As XRN1 is the only known enzyme with such activity in the cytoplasm of eukaryotic cells, it was logical to

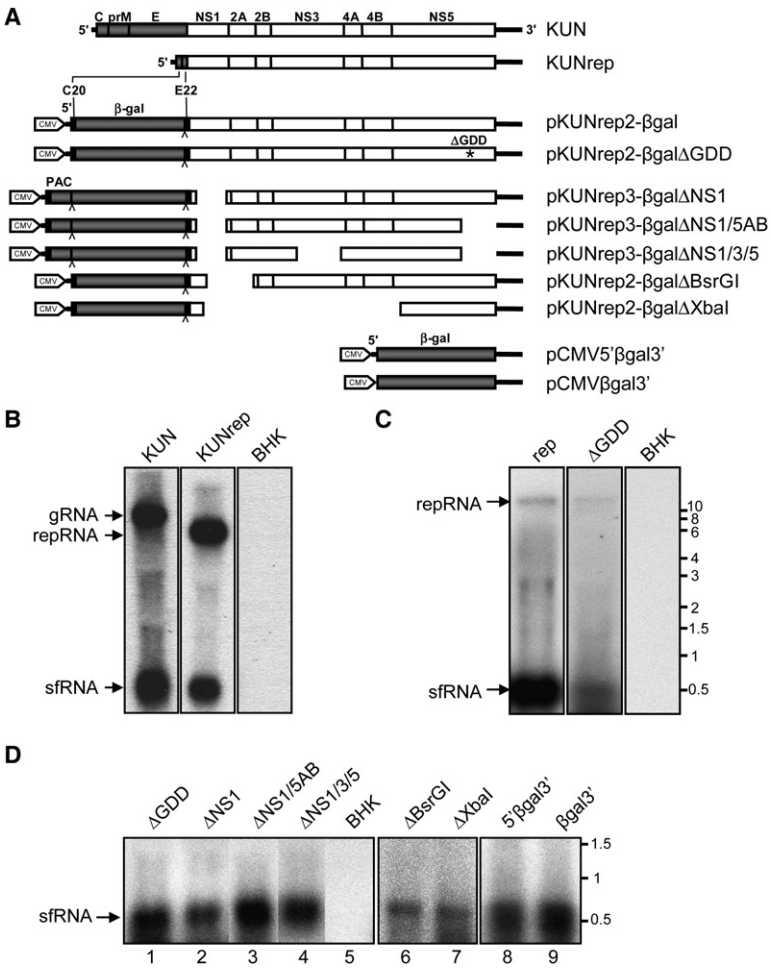

Figure 2. sfRNA Production Is Independent of RNA Replication, Viral Proteins, or 5′UTR

(A) Schematic representation of WNV_{KUN} (KUN) and replicon (KUNrep) genome organization as well as CMV-promoter-driven WNV_{KUN} replicon plasmids containing various deletions. Only KUN, repKUN, and pKUNrep2-βgal constructs produce replicating RNA; remaining constructs produce nonreplicating RNAs. C20, 20 amino acids from Core gene; β-gal, β-galactosidase reporter gene; E22, 22 amino acids from E gene; PAC, puromycin N-acetyltransferase gene.

(B) Northern blot of RNA isolated from BHK-21 cells infected with WNV_{KUN} or electroporated with WNV_{KUN} replicon RNA.

(C) Northern blot of RNA from BHK-21 cells transfected with pKUNrep2-βgal or pKUNrep2-βgalΔGDD. An RNA size marker is indicated (kb).

(D) Northern blot of RNA isolated from BHK-21 cells transfected with replicon constructs containing various deletions. A radiolabeled 3′UTR probe was used for all northern blots. repRNA, replicon RNA.

assume that it may be involved in sfRNA generation. To test this hypothesis, we analyzed the effect of XRN1 depletion by siRNA on sfRNA generation in virus-infected cells. Depletion of XRN1 in two different cell lines, A549 and SVGA (by about 90% and 67%, respectively), resulted in a significant decrease in the amount of sfRNA (by 56% and 47%, respectively) compared to cells transfected with control siRNA (Figure 3A). In another XRN1 depletion experiment in A549 cells, sfRNA was reduced by 52%. Statistical analysis of sfRNA production after XRN1 knockdown in these three independent experiments showed that sfRNA was reduced by 51.7% ± 4.5%. Thus, the results demonstrate reproducible downregulation of sfRNA production in XRN1-depleted cells.

Combined FISH and immunofluorescence analysis showed that viral 3′UTR-containing RNA partially colocalized with XRN1 in PBs of WNV_{KUN}-infected cells (Figure 3B). Later (30 hr) in infection, 22% ± 7% of RNA-labeled foci overlapped with XRN1-containing foci (right panels in Figure 3B). In contrast, staining of SFV-infected cells for SFV RNA and XRN1 showed no SFV RNA in PBs (Figure 3C). The siRNA depletion and colocalization results suggest that XRN1 is likely to be involved in sfRNA generation and that this process may occur in PBs. To determine whether sfRNA is indeed resistant to XRN1 degradation, we performed in vitro digestion of total RNA isolated from WNV_{KUN}-infected cells with recombinant XRN1. This enzyme was able to completely degrade RNA substrates from SFV and HCV (data not shown). In contrast, sfRNA was shown to be resistant to XRN1 treatment (Figure 3D), while it was readily degraded by treatment with other RNases, namely RNaseA and RNaseONE (Figure 3D). The results indicate that XRN1 is unable to degrade sfRNA and further implicate that sfRNA may be a product of XRN1 stalling.

Mapping of sfRNA and RNA Structure Predictions

Northern hybridization mapping of RNA isolated from WNV_{KUN}-infected cells with radiolabeled probes specific for different regions of the 3′UTR demonstrated that sfRNA corresponds to the last part of the 3′UTR (Figures S2A and S2B). Primer extension analysis showed that sfRNA isolated from WNV_{KUN} and WNV_{NY99}-infected cells or isolated from infected mouse brain had a size of 525 nt (Figure S2C).

Flavivirus 3′UTR has a number of characteristic features (Figure 4A), including an AU-rich region at the 5′ end, a number of conserved (repeated) sequences (CS1/2/3 and RCS2/3), a cyclization sequence, putative RNA pseudoknots (PKs), a pentanucleotide, and a conserved stem-loop structure at the 3′ terminus (3′SL) (Markoff, 2003). Using RNA structure prediction on a 3′UTR sequence alignment of different flaviviruses, we predicted a common RNA structure (designated SL-II) with remarkable similarity in overall architecture between the different viruses (Figure 4B). The high conservation of this complex RNA structure and location of the sfRNA 5′ end at its base suggest that this structure may be involved in protecting downstream 3′UTR RNA from degradation. Indeed, sfRNA sizes of 525 nt for WNV_{KUN} and WNV_{NY99} (Figure 1A), 521–523 nt for JEV (Lin et al., 2004), 0.5 kb for MVEV (Urosevic et al., 1997) and ALFV (Figure 1A), 0.4 kb for DENV2 (Figure 1A), and 0.3 kb for YFV (Figure 1A) correspond well to the respective locations of SL-II (SL-E in YFV) in the 3′UTRs (Figure 4B). The SL-II structure is remarkably similar to the previously predicted SL-IV structure

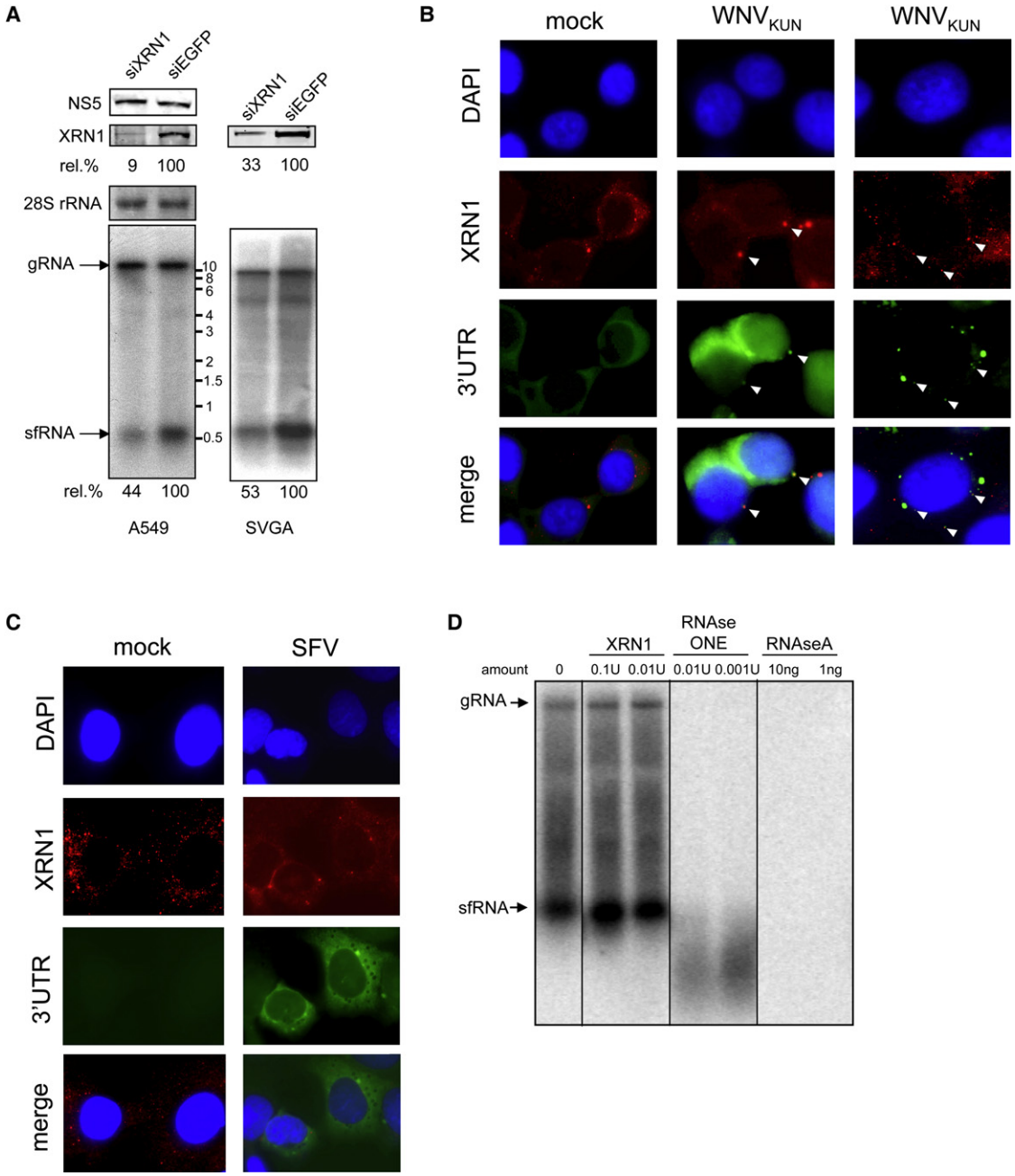

Figure 3. sfRNA Is Reduced in XRN1-Depleted WNV$_{KUN}$-Infected Cells, Colocalizes with XRN1 in Processing Bodies, and Is Resistant to XRN1 Degradation

(A) XRN1 depletion leads to decrease in sfRNA production in A549 and SVGA cells. (Top) Western blot detection of XRN1 and KUN NS5 proteins at 24 h.p.i. Rel. % represents percentage of XRN1 expression in cells treated with siRNA against XRN1 (siXRN1) compared to that in cells transfected with control siRNA (siEGFP). (Bottom) Northern blot with radiolabeled 3′UTR probe to quantify sfRNA (%) in XRN1-depleted cells. A representative of two independent experiments for A549 cells is shown.

(B) XRN1 colocalization with flavivirus 3′UTR. WNV$_{KUN}$-infected A549 cells were analyzed for viral RNA localization by FISH using FITC-labeled, 3′UTR-specific RNA probe and for XRN1 by immunofluorescence staining. Middle panels show labeling at 24 h.p.i.; right panels at 30 h.p.i. Arrows indicate colocalization.

(C) SFV-RNA does not colocalize with XRN1. SFV-infected A549 cells were analyzed as described above using a FITC-labeled 3′UTR SFV-RNA probe.

(D) Resistance of sfRNA to digestion with 5′-3′ exoribonuclease XRN1. RNA isolated from WNV$_{KUN}$-infected BHK-21 cells was digested with the indicated nucleases, followed by northern blotting and hybridization with radiolabeled 3′UTR probe.

(Proutski et al., 1997) located ~160 nt downstream of the beginning of the SL-II structure. Both WNV SL-II and SL-IV are followed by short conserved hairpins previously designated RCS3 and CS3, respectively (Figure 4A) (Khromykh and Westaway, 1994). Sequence alignment of SL-II and SL-IV of WNV$_{KUN}$, WNV$_{NY99}$, JEV, MVEV, ALFV, DENV2, and SL-E of YFV (Proutski

et al., 1997) showed conservation of a number of regions (Figure S3) that appear to form the backbone of the predicted SL-II (SL-E) and SL-IV RNA structures (Figure 4B).

RNA Structure/Sequence Requirements for sfRNA Generation

To experimentally determine the RNA structure responsible for protection of 3′UTR from degradation, we generated an extensive series of recombinant viruses with various deletions and mutations in the 3′UTR (Figure 4C) and determined their effect on sfRNA generation in infected cells (see Supplemental Data for more detailed description). Northern blot analysis showed that deletions/mutations in SL-II, as expected, resulted in the loss of full-length sfRNA (termed sfRNA1) (Figure 4D), supporting its essential role in sfRNA production. Additional deletions downstream of SL-II led to the production of two smaller, less abundant sfRNA species termed sfRNA2 and sfRNA3 (Figure 4D), suggesting that two additional rigid secondary/tertiary RNA structures downstream of SL-II, likely to be SL-IV and DB1 (Figure 4A), can protect WNV_{KUN} RNA from complete degradation. Importantly, plaque size and virus growth in mammalian and mosquito cells correlated with the generation and amount of full-length sfRNA1 (Figures 4E and 4F), showing that production of abundant amounts of full-length sfRNA1 is essential for efficient viral replication.

To confirm the uniqueness of flavivirus 3′UTR RNA structure(s) in the ability to protect from degradation, another highly structured RNA, internal ribosomal entry site (IRES) from encephalomyocarditis virus (EMCV) followed by neomycin transferase sequence (neo), was inserted upstream of SL-II in the 3′UTR of the WNV replicon WN-NeoRep (Shi et al., 2002) (Figure S4A), and cells stably expressing this replicon were generated by selection with G418. When total RNA isolated from these cells was subjected to northern blot analysis with 3′UTR-specific probe, only sfRNA1, but no other larger RNA-encompassing IRES-neo insertion, was detected (Figure S4B), demonstrating that the 5′ end of sfRNA1, but not the IRES structure, prevents degradation. This provides additional evidence for the uniqueness of flavivirus 3′UTR structure(s) in their ability to protect downstream RNA sequences from degradation.

sfRNA Production Is Required for Viral Cytopathicity in Cell Culture

To further characterize sfRNA function, a mutant virus not capable of producing sfRNA1 and sfRNA2 with minimal changes in RNA structure, FL-IRAΔCS3 was constructed. The mutations consisted of a 3 nt substitution in the IRA within SL-II and a 10 nt deletion of the CS3 sequence (ΔCS3) downstream of SL-IV (Figure 4C). As shown above, IRA mutation abolished sfRNA1 production (Figure 4D, lane 15), while ΔCS3 mutation abolished sfRNA2 production (Figure 4D, lane 9). The mutant virus with combined IRAΔCS3 mutations showed a severe defect in the production of sfRNA1 (Figure 5A, lanes 5 and 6), no visible plaque formation in Vero cells (Figure 5B), and decreased replication efficiency in mammalian (Vero) and mosquito (C6/36) cells (Figures 5C and 5D). However, maximum differences in virus titers were only about 5- to 10-fold. The mutant FL-IRA containing only 3 nt substitution in SL-II abolishing sfRNA1 production was also compromised in the ability to form clearly visible plaques (Figure 5B), but not so much in replication efficiency (Figures 5C and 5D). The mutations/deletions did not have a major effect on RNA translation, replication, or packaging efficiencies when introduced into replicon RNAs (Figure S5). To analyze the apparent discrepancy between dramatic differences in plaque morphology and only moderate differences in virus growth kinetics, mutant viruses were investigated for induction of cytopathicity. The number of viable cells was significantly higher in wells infected with FL-IRA and FL-IRAΔCS3 compared to FLSDX and FLΔCS3 (Figure 6A). Quantification analysis using released crystal violet stain showed clear differences in cytopathic effect (CPE) with about 70% of cells dead at 6 days postinfection (d.p.i.) with FLSDX and only 10% or less of cells dead after infection with either FL-IRA or FL-IRAΔCS3 mutants (Figure 6B). This difference in viral cytopathicity was confirmed by measuring the release of lactate dehydrogenase (LDH) by dying cells into the cell culture supernatant (Figure 6C).

To investigate whether sfRNA production alone induces cell death, the plasmid pCMVβgal3′ producing sfRNA without other viral components was transfected, and cell death was assessed by LDH release. sfRNA production alone did not lead to significant cell death (Figure 6D), indicating that sfRNA must act in the context of viral infection to promote virus-induced cytopathicity.

In order to confirm the role of sfRNA in virus-induced cytopathicity, the defect in sfRNA production was complemented by providing sfRNA1 in *trans* from transfected pCMVβgal3′. The cytopathicity of FL-IRAΔCS3 was, indeed, partially rescued in cells producing sfRNA from the transfected plasmid as determined by LDH release (Figure 6E). This was confirmed by the detection of more clear plaques in cells transfected with pCMVβgal3′ and infected with FL-IRAΔCS3 than in infected cells transfected with the control pCMVβgal (Figure 6F). In addition, viral titers were significantly increased in cells transfected with pCMVβgal3′ and infected with FL-IRAΔCS3 compared to those in infected cells transfected with the control plasmid (Figure 6G). In these experiments, transfection efficiency was between 50% and 60%, while 100% of cells were infected as determined by X-gal staining and immunofluorescence analyses, respectively (data not shown). Thus, the relatively inefficient but significant complementation can be explained by the limited transfection efficiency of the plasmid supplying the complementing sfRNA. Overall, the results demonstrate that production of abundant amounts of sfRNA1 during virus infection is a determinant of viral cytopathicity in cell culture.

sfRNA1 Is Required for Viral Pathogenicity in Mice

To investigate the effect of altered sfRNA production on viral pathogenicity in vivo, FLSDX, FL-IRA, FLΔCS3, and FL-IRAΔCS3 were injected in 3-week-old mice, a highly sensitive animal model for WNV_{KUN} infection. Mice infected with the wild-type virus FLSDX started to develop severe symptoms as early as day 6 after injection, and all animals had to be sacrificed 9 days after injection (Figure 7A). Mice injected with FLΔCS3, which produces less sfRNA1, developed symptoms after 7 days, with a mortality rate of 60% throughout the observation period (Figure 7A). In contrast, mice injected with either FL-IRA or FL-IRAΔCS3 showed no signs of WNV_{KUN}-induced encephalitis during the observation period (Figure 7A). Kinetic analysis of virus accumulation in the spleen and brain of infected mice

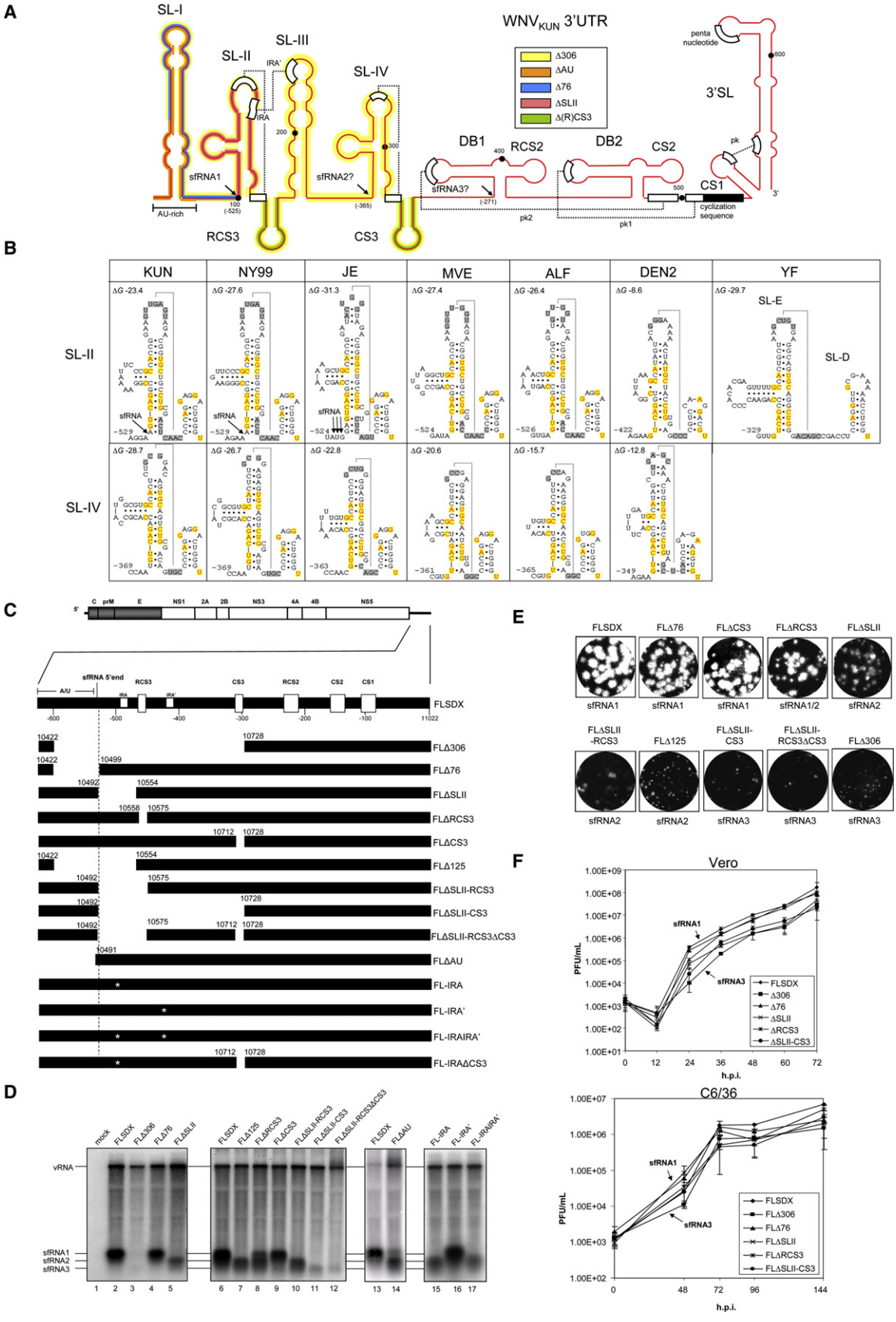
A
SL-I
SL-II
SL-III
SL-IV
IRA'
IRA
sfRNA1
sfRNA2?
sfRNA3?
AU-rich
RCS3
CS3
WNV$_{KUN}$ 3'UTR
Δ306
ΔAU
Δ76
ΔSLII
Δ(R)CS3
penta nucleotide
3'SL
DB1
RCS2
DB2
CS2
CS1
pk
pk2
pk1
cyclization sequence
B
KUN
NY99
JE
MVE
ALF
DEN2
YF
SL-II
SL-IV
SL-E
SL-D
C
FLSDX
FLΔ306
FLΔ76
FLΔSLII
FLΔRCS3
FLΔCS3
FLΔ125
FLΔSLII-RCS3
FLΔSLII-CS3
FLΔSLII-RCS3ΔCS3
FLΔAU
FL-IRA
FL-IRA'
FL-IRAIRA'
FL-IRAΔCS3
D
mock
vRNA
sfRNA1
sfRNA2
sfRNA3
E
FLSDX
FLΔ76
FLΔCS3
FLΔRCS3
FLΔSLII
FLΔSLII-RCS3
FLΔ125
FLΔSLII-CS3
FLΔSLII-RCS3ΔCS3
FLΔ306
F
Vero
C6/36
PFU/mL
h.p.i.
ΔRCS3
ΔSLII-CS3

demonstrated that all four viruses replicated in vivo with the sfRNA mutant viruses being detected in the brain later in infection at levels similar to corresponding parental viruses (i.e., FLSDX for FL-IRA and FLΔCS3 for FL-IRAΔCS3; Figures 7B and 7C). The results show that the production of sfRNA1 is not essential for viral replication and spread in vivo, while it has a crucial role in determining viral pathogenicity.

DISCUSSION

We demonstrated that all representative viruses from the genus Flaviviruses, but not from other genera of the *Flaviviridae* family, produce an abundant, subgenomic, noncoding RNA derived from the 3′UTR of gRNA. We have shown that RNA replication, viral proteins, or 5′UTR are not essential for generation of this subgenomic flavivirus RNA (sfRNA). We have provided evidence that sfRNA is a product of incomplete degradation of gRNA, which is likely to involve cellular 5′-3′ exoribonuclease XRN1, one of the key enzymes in the cellular mRNA decay pathway. In agreement with the high level of conservation between factors and pathways involved in mRNA decay of mosquito and human cells (Opyrchal et al., 2005), sfRNA was produced in cells of different origin, including mosquito cells.

In general, mRNA decay in the cell can follow different pathways. It can be regulated by decapping, deadenylation, translation, *cis*-acting elements, and "nonsense" sequences and has been shown to be a critical control point for determination of transcript abundance (Wilusz et al., 2001). 5′-3′ mRNA degradation takes place in PBs, which contain most enzymes and proteins needed for the basic decay machinery (Newbury et al., 2006). Our viral RNA and XRN1 colocalization results suggest that XRN1-mediated production of sfRNA in infected cells is likely to take place in PBs. However, it remains elusive how and why the viral genomic RNA is targeted to this RNA decay pathway. It is possible that viral gRNA molecules containing nonsense mutations and, thus, not being able to participate in translation, replication, or packaging can be targeted to PBs for degradation. Once in the PB, gRNA can be decapped and then degraded by XRN1 until the enzyme is stalled on rigid structures in the beginning of 3′UTR, ultimately resulting in production of sfRNA. The resistance of sfRNA to degradation by XRN1 shown here by in vitro digestion of viral RNA from infected cells using recombinant XRN1 supports this hypothesis. However the role of other ribonucleases present in infected cells in the generation of nuclease-resistant sfRNA cannot be ruled out. A recent study with a segmented positive-strand RNA virus from plants described generation of nuclease-resistant small noncoding RNA derived from the 3′UTR of one of the two viral RNAs via incomplete degradation of gRNAs (Iwakawa et al., 2008). Although the exclusive role of XRN1 in its generation was not demonstrated, several lines of evidence implicated the role of a cellular enzyme with 5′-3′ exoribonuclease activity in this process. These results provide additional support for our findings and further strengthen our hypothesis on the involvement of XRN1 in sfRNA generation.

The reason why sfRNA production is specific to the flavivirus genus of the *Flaviviridae* family and does not occur during infection with viruses from other genera (i.e., Pesti- and Hepaciviruses) is not entirely clear. The absence of small RNA in cells containing replicating SFV, HCV, and BVDV RNAs suggests that these RNAs do not contain structures able to protect against ribonuclease degradation. In support of the notion that not any but specifically flavivirus RNA structures are able to inhibit degradation, the highly structured IRES from EMCV, inserted upstream of the sfRNA 5′ end of WNV_{NY99} replicon, was not able to do so. Thus, contrary to the current view that the variable 5′ part of the flavivirus 3′UTR serves only as a spacer to secure proper RNA folding of the conserved 3′ end of the 3′UTR (Proutski et al., 1999), we now provide compelling experimental evidence that the 5′ part of the 3′UTR, in fact, harbors conserved RNA structures that play an essential role in the formation of sfRNA required for efficient virus replication and pathogenicity.

The important question is why flaviviruses evolved a strategy to generate sfRNA and how exactly it contributes to virus replication, cytopathicity, and pathogenicity. Subgenomic noncoding RNAs are only produced by a small number of other RNA viruses (e.g., Soybean dwarf virus [Yamagishi et al., 2003], Barley yellow dwarf virus [Koev and Miller, 2000], Citrus tristeza virus [Ayllon

Figure 4. Production of sfRNA Species Is Determined by the Presence of Highly Structured RNA Sequences and Contributes to Virus Replication

(A) RNA structure model of WNV_{KUN} 3′UTR generated from previously described and newly predicted RNA structures. Positions of nucleotides (nt) from beginning of the 3′UTR and corresponding positions from the end of 3′UTR showing sfRNA 5′ ends (in brackets) are indicated. IRA, inverted repeat A; IRA′, inverted repeat A′; (R)CS3/2/1, (repeated) conserved sequence; DB1/2, dumbbell structures; SL, stem-loop structures. Experimentally determined 5′ end of sfRNA1 and predicted 5′ ends of sfRNA2 and sfRNA3 are indicated by arrows. Putative pseudoknot interactions are indicated by dashed lines. Colored regions show the location of introduced deletions.

(B) Secondary RNA structure predictions of SL-II and SL-IV regions (SL-E for YFV) for different flaviviruses generated from sequence alignment. The conserved RNA structure has the following properties: (1) sfRNA 5′ end (determined for WNV and JE) located at base of SL-II, (2) conserved base pairing sequences in base stem, (3) variable side stem-loop, (4) two conserved unbound C residues at the heart of the structure, (5) conserved base pairing sequences in top stem, (6) variable top loop with putative pseudoknot interaction (dashed lines with spacer sequence located between SL-II and RCS3 or SL-IV and CS3 or, in case of YFV, SL-E and SL-D). Nt numbering from the end of 3′UTR. sfRNA 5′ ends are indicated by arrows. Conserved nt are in red letters with yellow background. Nt with putative pseudoknot interactions between top loop and spacer between SL-II and RCS3 have gray background. ΔG values show free minimal energies.

(C) Schematic representation of the WNV_{KUN} genome organization, 3′UTR, and introduced deletions/mutations. sfRNA 5′ end at position −525 is indicated. Nt positions shown at start and end of deletions correspond to nt in the viral genomic sequence (GenBank accession number AY274504). Nt substitutions in inverted repeats are indicated with an asterisk.

(D) Northern blot of RNA isolated from BHK-21 cells infected with virus mutants. gRNA, viral genomic RNA; sfRNA, subgenomic flavivirus RNA.

(E) Plaque assays on Vero cells. Cells were fixed and stained with crystal violet 6 d.p.i. sfRNA species (1, 2, or 3) produced by individual virus mutants are indicated.

(F) Growth kinetics of mutant viruses in mammalian (Vero, upper panel) and mosquito (C6/36, lower panel) cells infected with MOI = 0.1.

Data are represented as average ± SD.

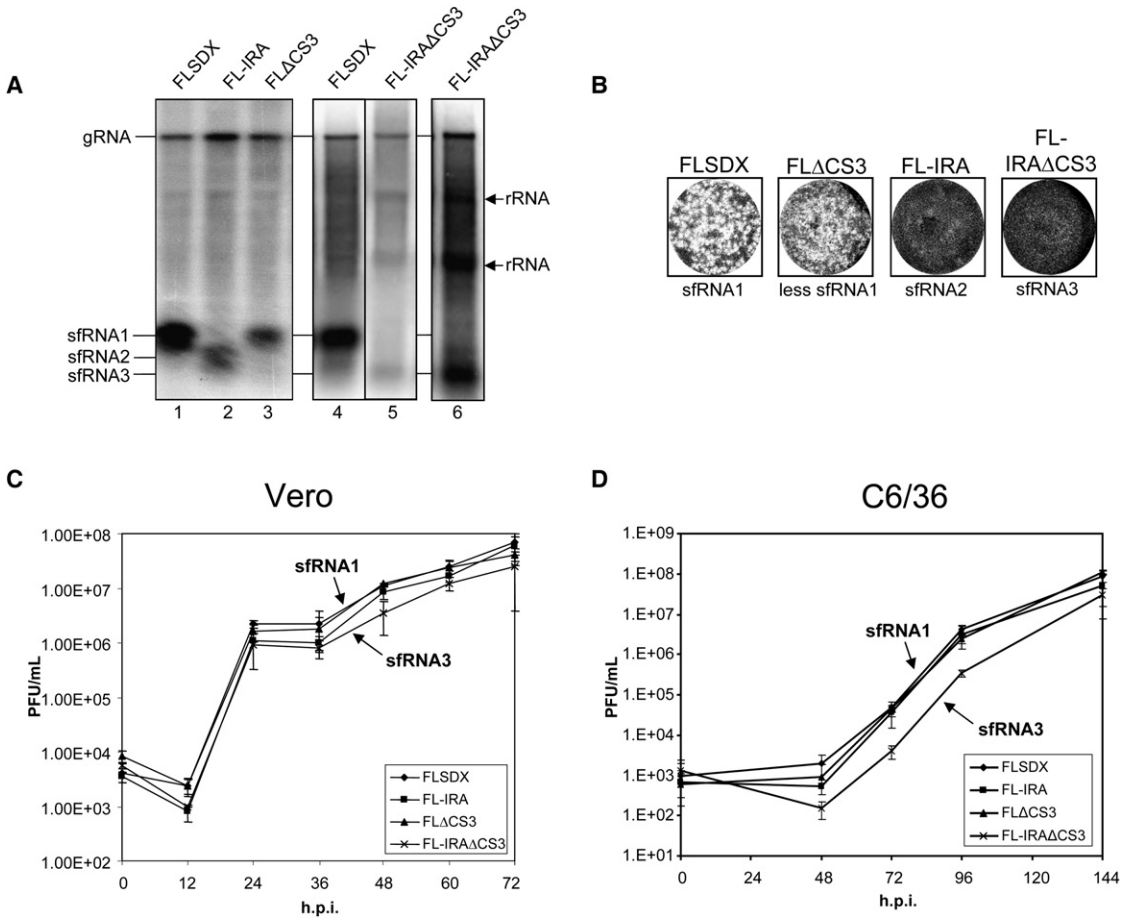

Figure 5. sfRNA1 Production Is Required for Efficient Virus Replication in Mammalian and Mosquito Cells

(A) Northern blot of RNA isolated from BHK-21 cells infected with virus mutants. Lane 6 shows a longer exposure of lane 5. gRNA, genomic RNA; sfRNA, subgenomic flavivirus RNA; rRNA, ribosomal RNA.

(B) Plaque assay on Vero cells. Cells were fixed and stained 6 d.p.i. sfRNA species (1, 2, or 3) produced by individual virus mutants is indicated.

(C) Virus growth kinetics in Vero cells infected with MOI = 1.

(D) Virus growth kinetics in mosquito C6/36 cells infected with MOI = 0.1.

Data are represented as average ± SD.

et al., 2004]), but their roles in viral replication or effects on the infected cell are still largely unexplored. Recent studies with plant RNA virus, Red clover necrotic mosaic virus, implicated a role for small noncoding RNA in regulating translation of viral proteins and negative-strain RNA synthesis but showed little effect of mutations ablating generation of this noncoding RNA on virus replication and pathogenicity in plants (Iwakawa et al., 2008). For flaviviruses, we have shown that the ability to produce full-length sfRNA is required for efficient virus growth and virus-induced cytopathicity in cell culture and pathogenicity in mice. This indicates that sfRNA may play a role in modulating the host antiviral response via RNA-mediated pathways. Cellular RNA sensors are responsible for recognition of foreign single-stranded and double-stranded RNAs and activation of signal pathways that ultimately lead to activation of the innate immune response or apoptosis (Yoneyama and Fujita, 2007). By binding and inactivating one of these sensors, sfRNA may prevent downstream signaling until viral replication is well established. Alternatively, sfRNA may act as a decoy for cellular miRNAs that may be induced by the antiviral response and might otherwise target viral RNA, as recently shown for HCV (Pedersen et al., 2007). In this scenario, sfRNA would prevent miRNA binding to gRNA and, thereby, prevent gRNA destruction. The impaired ability of sfRNA mutants to induce pathological changes in animals despite their demonstrated ability to reach and replicate in the brain after peripheral infection indicates that modulation of antiviral responses in the brain by sfRNA may be responsible for virus-induced pathogenicity. In addition, it has been shown that the cellular mRNA decay machinery can have antiviral function (Esteban et al., 2008) and may help to prevent recombination of viral RNA (Cheng et al., 2006). sfRNA may also function in inhibiting these activities.

The significantly impaired cytopathicity of viruses failing to produce sfRNA1 suggests that production of sfRNA1 contributes to the induction of cell death after infection. To date, cell death caused by flavivirus infection has been shown to be induced by replication and expression of viral proteins via a variety of pathways and mechanisms, including apoptosis and necrosis

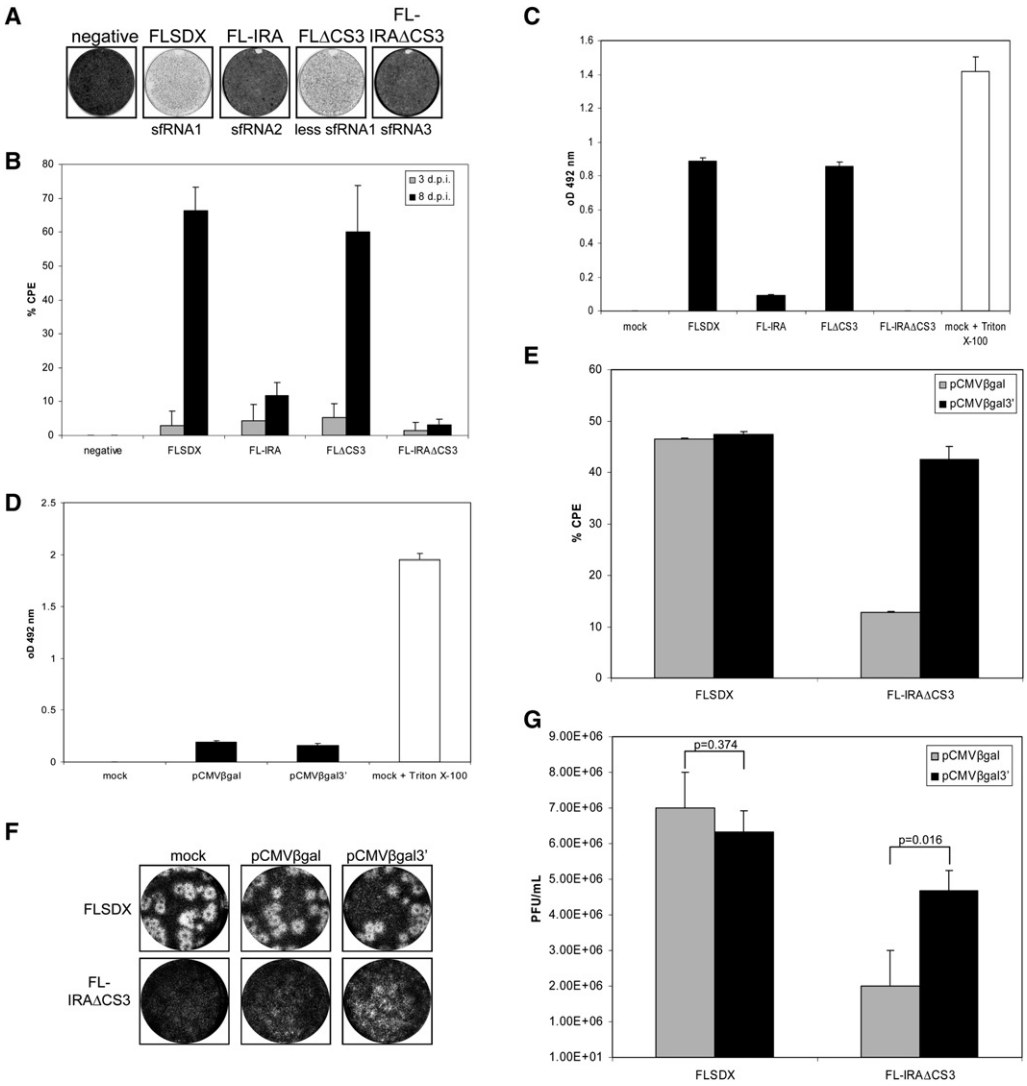

Figure 6. sfRNA1 Production Is Essential for Virus-Induced Cytopathicity

(A and B) Vero cells were infected and fixed at indicated time points after infection.

(A) Cells were stained 6 days after infection.

(B) Crystal violet was released from cells by methanol and OD 620 nm measured. Percentage of dead cells was calculated. CPE, cytopathic effect.

(C) LDH release into cell culture fluid of Vero cells infected with mutant viruses was measured 4 d.p.i. by colorimetric assay. Background from negative cells was subtracted. Percentage of dead cells was calculated.

(D) LDH release from Vero cells transfected with plasmid DNA producing sfRNA (pCMVβgal3′).

(E) Partial rescue of virus-induced cytopathicity by complementation with sfRNA. Vero cells were transfected with sfRNA-producing plasmid pCMVβgal3′ and control pCMVβgal. At 24 hr posttransfection, cells were infected with MOI = 1 FLSDX and FL-IRAΔCS3. LDH release was measured 8 d.p.i.

As a positive control for (C), (D), and (E), mock cells were lysed with 0.1% Triton X-100. Data are represented as average + SD.

(F) Partial rescue of viral plaque formation by sfRNA complementation. Vero cells were transfected with plasmids. At 24 hr later, cells were infected with corresponding viruses, overlayed with agarose, and stained 6 d.p.i.

(G) Partial rescue of virus production by sfRNA complementation.

Viral titers in culture fluid of DNA-transfected and virus-infected cells (as in [E]) were determined 48 hr after infection by plaque assay on BHK cells. P values were calculated by unpaired Student's t test.

(Ait-Goughoulte et al., 2007; Medigeshi et al., 2007; Ramanathan et al., 2006; Su et al., 2002; Yang et al., 2002). Interestingly, production of sfRNA1 alone without viral infection did not induce cell death, while it did complement the cytopathicity of viral mutants defective in sfRNA production, suggesting that viral factors and/or cellular factors induced by virus infection may be required for sfRNA-mediated cell death. Thus, sfRNA production might be a viral trigger to facilitate cell death; however, identification of the exact pathway and mechanisms by which sfRNA leads to cell death requires further experimentation.

In conclusion, we showed that all members of the genus Flavivirus encode unique RNA element(s) at the beginning of 3′UTR

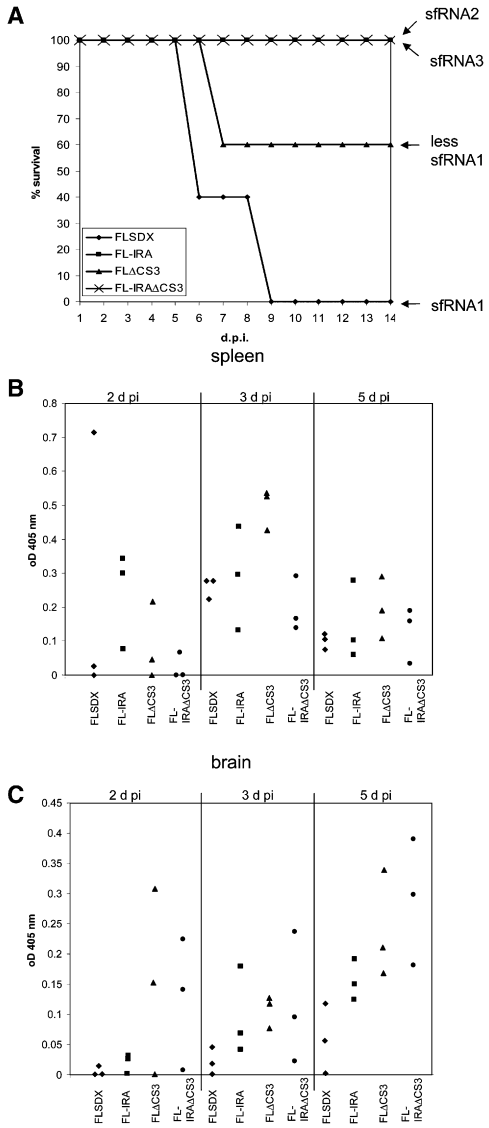

Figure 7. sfRNA1 Production Is a Determinant of Viral Pathogenicity in Mice

Three-week-old Swiss outbred mice (five per group) were i.p. injected with 10,000 PFU of virus. (A) Mice were monitored daily and sacrificed when encephalitis symptoms became evident. As a control, five mice were injected with medium only. These mice remained healthy over the observation period (data not shown). Relative amounts of sfRNA and sfRNA species produced by the viruses are indicated. Spleens (B) and brain (C) were recovered from three infected mice per time point per group, and C6/36 cells were infected with corresponding homogenates. Presence of infectious virus in infected cells was determined by ELISA, and OD 405 nm was measured.

that are responsible for protection of downstream RNA from degradation by cellular ribonucleases. The resulting nuclease-resistant noncoding RNA product plays an important role in the virus replication cycle and contributes to viral cytopathicity and pathogenicity. In addition to the high potential of sfRNA mutants for the development of attenuated flavivirus vaccines, the strong influence of sfRNA on the viral life cycle can also provide a valuable tool to study cellular mechanisms of RNA turnover. Clear biological readout in the form of virus replication, virus-induced cytopathicity, and viral pathogenicity in laboratory animals may allow easy and reliable assessment of the effects of various factors on the biogenesis and functions of the cellular RNA decay machinery. Our findings offer valuable insight into the fields of virology and cell biology and provide significant contribution to the research concerning noncoding RNA-mediated mechanisms of viral pathogenicity and mechanisms of cellular RNA decay.

EXPERIMENTAL PROCEDURES

Construction of Mutant Viruses and RNA Electroporation

WNV_{KUN} full-length cDNA clone FLSDX (pro)_HDVr (designated FLSDX) was described previously (Liu et al., 2003). A XmaI-*Xho*I fragment from FLSDX (pro)_HDVr was cloned into pBluescript generating pBS-3′XX. Mutations and deletions in the WNV_{KUN} 3′UTR were engineered into pBS-3′XX using Quickchange PCR site-directed mutagenesis with primers listed (Table S1). Presence of mutations was confirmed by sequencing, and fragments were reinserted into FLSDX (pro)_HDVr. Full-length cDNA clones were linearized and purified. In vitro RNA transcription and electroporation of BHK-21 cells were performed as described previously (Khromykh and Westaway, 1997). Recovered viruses were amplified on BHK-21 cells to generate virus stocks. Virus titers were determined by standard plaque assay on BHK-21 cells. Viral RNA was isolated from virus stocks, amplified by RT-PCR, and sequenced to confirm presence of the mutations. Virus stocks were stored in 0.5 ml aliquots at –80°C.

Plasmid Construction and DNA Transfection

pKUNrep2-βgal, pKUNrep2-βgalΔGDD, and pKUNrep3-βgal were described previously (Varnavski et al., 2000). pKUNrep3-βgalΔNS1, pKUNrep3-βgalΔNS1/5AB, and pKUNrep3-βgalΔNS1/3/5 were created essentially as described (Khromykh, 2000). pKUNrep2-βgalΔBsrGI and pKUNrep2-βgalΔXbaI were created by deleting *Bsr*GI and *Xba*I fragments from pKUNrep2-βgal, respectively. Although these replicon constructs are defective in RNA replication, translation of the encoded polyprotein was efficient (data not shown). pCMV5′βgal3′ and pCMVβgal3′ were created by PCR-directed deletion mutagenesis with overlapping primers (Table S1) using pKUN1 (Khromykh et al., 2001) as a template. The βgal gene from repPAC-βgal (Liu et al., 2002) was subsequently inserted as an *Nsi*I fragment. DNA transfection was carried out using Lipofectamine (Invitrogen) following the manufacturer's protocol.

Virus Infection, Growth Kinetics, and Plaque Assay

Vero and C6/36 cells were infected at a multiplicity of infection (MOI) of 0.1 to 1 for 2 hr at 37°C, washed three times with PBS, and overlaid with DMEM containing 2% FBS. For growth curves, cell culture fluid from 6-well plates was harvested at the indicated times postinfection to determine virus titers by standard plaque assay on BHK-21 cells. For plaque assays, BHK-21 or Vero cells in 6-well plates were infected with a dilution series of viruses as described above. Cells were overlaid with 0.75% LMP agarose in DMEM containing 2% FCS, incubated at 37°C for 4 (BHK-21) or 6 (Vero) days, fixed with 10% formaldehyde, and stained with 0.2% crystal violet.

RNA Isolation and Northern Hybridization

Mouse brain tissue infected with WNV_{KUN} strain MRM61C (Khromykh and Westaway, 1994) was used as a source for RNA extraction. WNV_{KUN} virions (generated from FLSDX) were purified from culture fluid of infected BHK cells by continuous sucrose gradient (5%–25% w/v) and tested for infectivity by plaque assay. RNA was isolated with Trizol (Invitrogen) following the manufacturer's recommendations. Total RNA from Huh-7 cells transfected with HCV replicon C5B was a gift from Dr. Michael Beard.

Total RNA (10 μg) was subjected to denaturing gel electrophoresis in a 1.5% agarose, 2% formaldehyde gel followed by transfer onto Hybond-N membranes (Amersham, Buckinghamshire, UK). Membranes were dried, RNA crosslinked by UV-irradiation for 2 min, and hybridized for 1 hr with [^{32}P]-labeled (Perkin Elmer, Waltham, USA) 3′UTR probes in ExpressHyb solution (Clontech, Mountain View, USA) following the manufacturer's

recommendations. Blots were exposed on Kodak Biomax MS film or a phosphorscreen, and signals were quantified using a Typhoon phosphorimager (Amersham).

Nuclease Assays

RNA isolated from infected BHK cells was digested with the indicated amount of XRN1 (Epicenter, Madison, USA), RNaseONE (Promega), or RNaseA (Epicenter) for 30 min at 30°C and prepared for northern hybridization.

siRNA Knockdown of XRN1 and Western Blotting

A549 or SVGA cells were seeded in 6-well plates and transfected three times with 24 hr intervals using Lipofectamine 2000 (Invitrogen) and 20 pmol of a mixture of three Stealth siRNAs against human XRN1 or Stealth siRNA against eGFP (Invitrogen) following the manufacturer's protocol. Proteins were separated in 12.5% SDS-PAGE gels and transferred to Hybond ECL membranes (Amersham). Immunodetection was performed with a cocktail of mouse monoclonal antiserum against NS5 (1:200) and a rabbit polyclonal antiserum against human XRN1 (1:1000; Novus Biologicals, Littleton, USA). Secondary antibodies were IRdye800 anti-rabbit (1:5000; Rockland Immunochemicals, Gilbertsville, USA) and AlexaFluor680 anti-mouse (1:5000; Molecular Probes, Carlsbad, USA). Dried blots were scanned on an Odyssey infrared imager (LI-COR Biosciences, Lincoln, USA).

Fluorescent In Situ Hybridization and Immunofluorescence Analyses

The FITC-labeled, 3′UTR-specific probe was generated by in vitro transcription using T3 RNA polymerase, pBS-3′XX plasmid described above, and a fluorescein RNA labeling mix (Roche, Australia). After transcription, alkali hydrolysis was performed. To generate SFV 3′UTR probe, RNA isolated from SFV-infected cells was subjected to RT-PCR specific for the 3′UTR with a Sp6 promoter-containing primer. This PCR product was used for in vitro transcription with Sp6 polymerase as above.

A549 cells were seeded on coverslips and infected with FLSDX at MOI = 2 as described above. At 24 or 30 hr after infection, cells were fixed with 4% paraformaldehyde and permeabilized with 0.2% Triton X-100. FISH probe was diluted 1:100 in hybridization buffer, and coverslips were incubated with the probe overnight at 45°C. Coverslips were washed with 0.1 × SSC and PBS and incubated with rabbit anti-XRN1 antibody (1:500), which was detected with an AlexaFluor549 anti-rabbit antibody (Molecular Probes). Nuclei were counterstained with DAPI. Pictures were acquired using a Zeiss Axiophot 2 microscope equipped with an AxioCam MRm camera and AxioVision AC software. The percentage of colocalization at 30 hr postinfection (h.p.i.) was calculated as the average percentage ratio of dually labeled (yellow) spots to FISH-labeled (green) spots in five different areas on two different coverslips. For SFV-FISH, A549 cells were infected at MOI = 1 and stained 24 h.p.i as described above.

RNA Structure Prediction and Modeling

A secondary structure model of the entire WNV_{KUN} 3′UTR was generated based on a previously generated cotranscriptional model of the 3′UTR (Proutski et al., 1999) from RCS3 onward using the STAR program (Gultyaev et al., 1995; van Batenburg et al., 1995). Similar folds of the dumbbell structures containing RCS2/CS2 with putative pseudoknots pk2 and pk1 (Olsthoorn and Bol, 2001) and the 3′SL (Hahn et al., 1987; Shi et al., 1996; Wengler and Castle, 1986) were published previously. The SL-I structure at the 5′ end of the 3′UTR was generated using Mfold (this study). A common structure prediction for aligned SL-II and SL-IV sequences was generated by Pfold (Knudsen and Hein, 2003). Free energy values of individual SL-II and SL-IV structures were calculated by Mfold using forced base pairing. Putative pseudoknot interactions were located manually.

Cytopathicity and Complementation Assays

Vero cells were seeded into 24-well plates and infected with MOI = 0.1 as described above. At 3 to 8 days after infection, CPE was assessed as described previously (Liu et al., 2006). LDH release from cells was measured with Cytotoxicity Detection Kit (Roche, Mannheim, Germany) according to the manufacturer's instructions.

To assess cytotoxicity of sfRNA expressed from plasmid DNA, Vero cells were transfected with 500 ng pCMVβgal3′, and control pCMVβgal plasmid and cell culture supernatant was harvested for LDH assay 48 hr after transfection. Transfection efficiency determined by X-gal staining was between 50% and 60%. To complement sfRNA, Vero cells plated at a density of about 50% were transfected with 500 ng pCMVβgal3′ and control pCMVβgal. At 24 hr after transfection, cells were infected with FLSDX and FL-IRAΔCS3 at MOI = 1. At 8 days after infection, cell culture supernatant was harvested and LDH release measured. In parallel, supernatant from transfected and infected cultures was harvested 48 hr after infection and viral titers determined by plaque assay. To assess plaque formation after transfection, cells in 6-well plates were transfected with 1.5 μg DNA/well and infected 24 hr later for plaque assay as described above.

Mouse Virulence Study and Determination of Viral Burden

Groups of five mice were injected intraperitoneally with 10,000 plaque-forming units (PFU) of the different viruses in DMEM. As control, five mice were injected with DMEM. Mice were monitored for 14 days three times per day for clinical symptoms of WNV infection (ruffled fur, antisocial behavior, paralysis, hunched posture). Mice that showed clear symptoms of encephalitis were euthanized. For the analysis of viral burden in brain and spleen of infected mice, organs from three mice each were recovered at days 2, 3, and 5 after infection, weighed, and homogenized in medium using beads. Homogenate was centrifuged, and supernatant was used to infect duplicate wells of C6/36 cells. The presence of virus was determined by ELISA 7 days after infection using monoclonal anti-E antibodies as described previously (Hall et al., 2003). The experiments were conducted with approval from the University of Queensland Animal Experimentation Ethics Committee in accordance with the guidelines for animal experimentation as set out by the National Health and Medical Research Council, Australia.

SUPPLEMENTAL DATA

The Supplemental Data include Supplemental Text, Experimental Procedures, one table, and five figures and can be found with this article online at http://www.cellhostandmicrobe.com/supplemental/S1931-3128(08)00334-X.

ACKNOWLEDGMENTS

The authors would like to thank Wai Yuen Cheah for providing PS-EK cells and flavivirus isolates YFV, MVEV, ALFV, and SREV. We acknowledge Tim Mahoney for providing RNA from BVDV-infected MDBK cells, Andrew Davidson for providing DENV2 replicon, and Michael Beard for providing RNA samples from HCV replicon-transfected cells. Xiang Ju Wang is acknowledged for technical assistance and Hedije Meka for initial sfRNA mapping. Finally, we thank Edwin Westaway and Jason Mackenzie for helpful discussions. We are grateful to Roy Parker for critical reading of the manuscript and valuable comments.

This work was supported by grants to A.A.K. from the National Health and Medical Research Council of Australia.

Received: March 10, 2008
Revised: June 10, 2008
Accepted: October 15, 2008
Published: December 10, 2008

REFERENCES

Ait-Goughoulte, M., Kanda, T., Meyer, K., Ryerse, J.S., Ray, R.B., and Ray, R. (2007). Hepatitis C virus genotype 1a growth and induction of autophagy. J. Virol. *82*, 2241–2249.

Ayllon, M.A., Gowda, S., Satyanarayana, T., and Dawson, W.O. (2004). cis-acting elements at opposite ends of the Citrus tristeza virus genome differ in initiation and termination of subgenomic RNAs. Virology *322*, 41–50.

Cheng, C.P., Serviene, E., and Nagy, P.D. (2006). Suppression of viral RNA recombination by a host exoribonuclease. J. Virol. *80*, 2631–2640.

Esteban, R., Vega, L., and Fujimura, T. (2008). 20S RNA narnavirus defies the antiviral activity of SKI1/XRN1 in Saccharomyces cerevisiae. J. Biol. Chem. *283*, 25812–25820.

Eulalio, A., Behm-Ansmant, I., and Izaurralde, E. (2007). P bodies: at the crossroads of post-transcriptional pathways. Nat. Rev. Mol. Cell Biol. *8*, 9–22.

Gultyaev, A.P., van Batenburg, F.H., and Pleij, C.W. (1995). The computer simulation of RNA folding pathways using a genetic algorithm. J. Mol. Biol. *250*, 37–51.

Hahn, C.S., Hahn, Y.S., Rice, C.M., Lee, E., Dalgarno, L., Strauss, E.G., and Strauss, J.H. (1987). Conserved elements in the 3′ untranslated region of flavivirus RNAs and potential cyclization sequences. J. Mol. Biol. *198*, 33–41.

Hall, R.A., Broom, A.K., Smith, D.W., and Mackenzie, J.S. (2002). The ecology and epidemiology of Kunjin virus. Curr. Top. Microbiol. Immunol. *267*, 253–269.

Hall, R.A., Nisbet, D.J., Pham, K.B., Pyke, A.T., Smith, G.A., and Khromykh, A.A. (2003). DNA vaccine coding for the full-length infectious Kunjin virus RNA protects mice against the New York strain of West Nile virus. Proc. Natl. Acad. Sci. USA *100*, 10460–10464.

Iwakawa, H.O., Mizumoto, H., Nagano, H., Imoto, Y., Takigawa, K., Sarawaneeyaruk, S., Kaido, M., Mise, K., and Okuno, T. (2008). A viral noncoding RNA generated by cis-element-mediated protection against 5′→3′ RNA decay represses both cap-independent and cap-dependent translation. J. Virol. *82*, 10162–10174.

Khromykh, A.A. (2000). Replicon-based vectors of positive strand RNA viruses. Curr. Opin. Mol. Ther. *2*, 555–569.

Khromykh, A.A., and Westaway, E.G. (1994). Completion of Kunjin virus RNA sequence and recovery of an infectious RNA transcribed from stably cloned full-length cDNA. J. Virol. *68*, 4580–4588.

Khromykh, A.A., and Westaway, E.G. (1997). Subgenomic replicons of the flavivirus Kunjin: construction and applications. J. Virol. *71*, 1497–1505.

Khromykh, A.A., Meka, H., Guyatt, K.J., and Westaway, E.G. (2001). Essential role of cyclization sequences in flavivirus RNA replication. J. Virol. *75*, 6719–6728.

Knudsen, B., and Hein, J. (2003). Pfold: RNA secondary structure prediction using stochastic context-free grammars. Nucleic Acids Res. *31*, 3423–3428.

Koev, G., and Miller, W.A. (2000). A positive-strand RNA virus with three very different subgenomic RNA promoters. J. Virol. *74*, 5988–5996.

Lin, K.C., Chang, H.L., and Chang, R.Y. (2004). Accumulation of a 3′-terminal genome fragment in Japanese encephalitis virus-infected mammalian and mosquito cells. J. Virol. *78*, 5133–5138.

Liu, W.J., Sedlak, P.L., Kondratieva, N., and Khromykh, A.A. (2002). Complementation analysis of the flavivirus Kunjin NS3 and NS5 proteins defines the minimal regions essential for formation of a replication complex and shows a requirement of NS3 in cis for virus assembly. J. Virol. *76*, 10766–10775.

Liu, W.J., Chen, H.B., and Khromykh, A.A. (2003). Molecular and functional analyses of Kunjin virus infectious cDNA clones demonstrate the essential roles for NS2A in virus assembly and for a nonconservative residue in NS3 in RNA replication. J. Virol. *77*, 7804–7813.

Liu, W.J., Chen, H.B., Wang, X.J., Huang, H., and Khromykh, A.A. (2004). Analysis of adaptive mutations in Kunjin virus replicon RNA reveals a novel role for the flavivirus nonstructural protein NS2A in inhibition of beta interferon promoter-driven transcription. J. Virol. *78*, 12225–12235.

Liu, W.J., Wang, X.J., Mokhonov, V.V., Shi, P.Y., Randall, R., and Khromykh, A.A. (2005). Inhibition of interferon signaling by the New York 99 strain and Kunjin subtype of West Nile virus involves blockage of STAT1 and STAT2 activation by nonstructural proteins. J. Virol. *79*, 1934–1942.

Liu, W.J., Wang, X.J., Clark, D.C., Lobigs, M., Hall, R.A., and Khromykh, A.A. (2006). A single amino acid substitution in the West Nile virus nonstructural protein NS2A disables its ability to inhibit alpha/beta interferon induction and attenuates virus virulence in mice. J. Virol. *80*, 2396–2404.

Markoff, L. (2003). 5′- and 3′-noncoding regions in flavivirus RNA. Adv. Virus Res. *59*, 177–228.

Medigeshi, G.R., Lancaster, A.M., Hirsch, A.J., Briese, T., Lipkin, W.I., Defilippis, V., Fruh, K., Mason, P.W., Nikolich-Zugich, J., and Nelson, J.A. (2007). West Nile virus infection activates the unfolded protein response, leading to CHOP induction and apoptosis. J. Virol. *81*, 10849–10860.

Newbury, S.F., Muhlemann, O., and Stoecklin, G. (2006). Turnover in the Alps: an mRNA perspective. Workshops on mechanisms and regulation of mRNA turnover. EMBO Rep. *7*, 143–148.

Olsthoorn, R.C., and Bol, J.F. (2001). Sequence comparison and secondary structure analysis of the 3′ noncoding region of flavivirus genomes reveals multiple pseudoknots. RNA *7*, 1370–1377.

Opyrchal, M., Anderson, J.R., Sokoloski, K.J., Wilusz, C.J., and Wilusz, J. (2005). A cell-free mRNA stability assay reveals conservation of the enzymes and mechanisms of mRNA decay between mosquito and mammalian cell lines. Insect Biochem. Mol. Biol. *35*, 1321–1334.

Pedersen, I.M., Cheng, G., Wieland, S., Volinia, S., Croce, C.M., Chisari, F.V., and David, M. (2007). Interferon modulation of cellular microRNAs as an antiviral mechanism. Nature *449*, 919–922.

Poole, T.L., and Stevens, A. (1997). Structural modifications of RNA influence the 5′ exoribonucleolytic hydrolysis by XRN1 and HKE1 of Saccharomyces cerevisiae. Biochem. Biophys. Res. Commun. *235*, 799–805.

Proutski, V., Gould, E.A., and Holmes, E.C. (1997). Secondary structure of the 3′ untranslated region of flaviviruses: similarities and differences. Nucleic Acids Res. *25*, 1194–1202.

Proutski, V., Gritsun, T.S., Gould, E.A., and Holmes, E.C. (1999). Biological consequences of deletions within the 3′-untranslated region of flaviviruses may be due to rearrangements of RNA secondary structure. Virus Res. *64*, 107–123.

Ramanathan, M.P., Chambers, J.A., Pankhong, P., Chattergoon, M., Attatippaholkun, W., Dang, K., Shah, N., and Weiner, D.B. (2006). Host cell killing by the West Nile Virus NS2B-NS3 proteolytic complex: NS3 alone is sufficient to recruit caspase-8-based apoptotic pathway. Virology *345*, 56–72.

Scherbik, S.V., Paranjape, J.M., Stockman, B.M., Silverman, R.H., and Brinton, M.A. (2006). RNase L plays a role in the antiviral response to West Nile virus. J. Virol. *80*, 2987–2999.

Sheth, U., and Parker, R. (2003). Decapping and decay of messenger RNA occur in cytoplasmic processing bodies. Science *300*, 805–808.

Shi, P.Y., Brinton, M.A., Veal, J.M., Zhong, Y.Y., and Wilson, W.D. (1996). Evidence for the existence of a pseudoknot structure at the 3′ terminus of the flavivirus genomic RNA. Biochemistry *35*, 4222–4230.

Shi, P.Y., Tilgner, M., Lo, M.K., Kent, K.A., and Bernard, K.A. (2002). Infectious cDNA clone of the epidemic west nile virus from New York City. J. Virol. *76*, 5847–5856.

Stevens, A. (2001). 5′-exoribonuclease 1: Xrn1. Methods Enzymol. *342*, 251–259.

Su, H.L., Liao, C.L., and Lin, Y.L. (2002). Japanese encephalitis virus infection initiates endoplasmic reticulum stress and an unfolded protein response. J. Virol. *76*, 4162–4171.

Tourriere, H., Chebli, K., and Tazi, J. (2002). mRNA degradation machines in eukaryotic cells. Biochimie. *84*, 821–837.

Urosevic, N., van Maanen, M., Mansfield, J.P., Mackenzie, J.S., and Shellam, G.R. (1997). Molecular characterization of virus-specific RNA produced in the brains of flavivirus-susceptible and -resistant mice after challenge with Murray Valley encephalitis virus. J. Gen. Virol. *78*, 23–29.

van Batenburg, F.H., Gultyaev, A.P., and Pleij, C.W. (1995). An APL-programmed genetic algorithm for the prediction of RNA secondary structure. J. Theor. Biol. *174*, 269–280.

Varnavski, A.N., Young, P.R., and Khromykh, A.A. (2000). Stable high-level expression of heterologous genes in vitro and in vivo by noncytopathic DNA-based Kunjin virus replicon vectors. J. Virol. *74*, 4394–4403.

Wengler, G., and Castle, E. (1986). Analysis of structural properties which possibly are characteristic for the 3′-terminal sequence of the genome RNA of flaviviruses. J. Gen. Virol. *67*, 1183–1188.

Westaway, E.G., Mackenzie, J.M., and Khromykh, A.A. (2002). Replication and gene function in Kunjin virus. Curr. Top. Microbiol. Immunol. *267*, 323–351.

Westaway, E.G., Mackenzie, J.M., and Khromykh, A.A. (2003). Kunjin RNA replication and applications of Kunjin replicons. Adv. Virus Res. *59*, 99–140.

Wilusz, C.J., Wormington, M., and Peltz, S.W. (2001). The cap-to-tail guide to mRNA turnover. Nat. Rev. Mol. Cell Biol. *2*, 237–246.

Yamagishi, N., Terauchi, H., Kanematsu, S., and Hidaka, S. (2003). Characterization of the small subgenomic RNA of Soybean dwarf virus. Arch. Virol. *148*, 1827–1834.

Yang, J.S., Ramanathan, M.P., Muthumani, K., Choo, A.Y., Jin, S.H., Yu, Q.C., Hwang, D.S., Choo, D.K., Lee, M.D., Dang, K., et al. (2002). Induction of inflammation by West Nile virus capsid through the caspase-9 apoptotic pathway. Emerg. Infect. Dis. *8*, 1379–1384.

Yoneyama, M., and Fujita, T. (2007). RIG-I family RNA helicases: cytoplasmic sensor for antiviral innate immunity. Cytokine Growth Factor Rev. *18*, 545–551.